



## Photo-thermal effect with photonic crystals for photocatalysis and water desalination

Ilka Kriegel<sup>a</sup>, Francesco Scotognella<sup>b,\*</sup>

<sup>a</sup> Functional Nanosystems, Istituto Italiano di Tecnologia, Via Morego 30, 16163, Genova, Italy

<sup>b</sup> Dipartimento di Fisica, Politecnico di Milano, Piazza Leonardo da Vinci 32, 20133, Milano, Italy

### ARTICLE INFO

#### Keywords:

Water desalination  
Photonic applications  
Photothermal effects  
Photonic heater

### ABSTRACT

The demand of water is absolutely important for irrigation, industrial processes and domestic use. An interesting strategy to cope with the increasing water need is water desalination, which can be pursued with several strategies. Usually, the energy requirement of desalination plants is rather high. Membrane distillation is a good alternative, but it requires a non negligible amount of energy to heat the input water. Photothermal effects that exploit photonic structures can overcome this problem. In this review, we report significant works that employ photonic devices for water desalination. Moreover, we envisage the use of low-cost and easy-to-design one-dimensional photonic crystals and random photonic structures as photothermal devices.

For billions of people around the world the availability of reliable sources of drinkable water is a challenge of global importance [1,2]. Moreover, the demand of water worldwide is expected to increase by 55% over the next thirty years and this will be due to population growth, climate change and augmented industrialization [3–5]. A growing population is tightly connected to the challenge to produce more food, which requires more water withdrawals for irrigation. It is noteworthy that irrigation accounts for 70% of water withdrawals, while the industrial sector accounts for 20% and the domestic sector accounts for 10% of water withdrawals, respectively [6,7].

An interesting way to cope with the increasing water demand is water desalination. Unfortunately, the energy need by the desalination plants is rather significant [8,9]. Membrane distillation is a good alternative, but requires energy to heat the input water [9,10]. To decrease the energy consumption of the membrane distillation-based water desalination, photonic strategies to exploit photothermal effects have been pursued. In this short review, we report several significant studies on photonic-related water desalination strategies.

In 2016 Zhou et al. have demonstrated a plasmon-enhanced water desalination device [11]. The device consists of three components: i) a nanoporous anodic aluminum oxide membrane, obtained by the anodic oxidation of an aluminum foil; ii) close-packed aluminum nanoparticles along the sidewalls of the pores; iii) a thin film of aluminum onto the anodic aluminum oxide membrane. Under solar illumination, the water steam at the water-air interface exits the water desalination device and

condenses in a condensation chamber [11]. The advantage of this structure is the strong light absorption all over the solar spectrum.

In 2017 Dongare et al. have demonstrated nanophotonics-enabled solar membrane distillation in which the nanophotonic structure leads to localized photothermal heating, induced by solar illumination, eliminating the requirement of heating the input water [9]. The same research group have developed properly designed nanostructured arrays that lead to a focus of solar illumination in “hot spots” [12]. Moreover, they have demonstrated that, in the desalination process, the heat exchange between distilled and input water can reach a resonant condition, dramatically enhancing the fresh water production [2]. Also the use of photonic crystals [13–15] can be beneficial for water desalination processes. In 2020, Sayed, Krauss, and Aly have simulated with finite element methods a two-dimensional photonic crystal, i.e. a two-dimensional array of titanium nitrate pyramids coated with titanium dioxide, which can show an efficient water desalination [16].

Haddad et al., in 2021 have demonstrated water desalination via forward osmosis employing thermally responsive ionic liquids. To provide heat to the system, a photonic heater, the converts sunlight into heat, has been used [5]. The experimental setup built by Haddad et al. is sketched in Fig. 1. Pre-treated produced water enters in a forward osmosis module that contains ionic liquid draw solute. The concentration of the ionic liquid draw solute is higher with respect to the feed. Water molecules diffuse through the membrane under a natural osmotic gradient. The diluted draw enters in the thermal separation module. The

\* Corresponding author.

E-mail address: [francesco.scotognella@polimi.it](mailto:francesco.scotognella@polimi.it) (F. Scotognella).

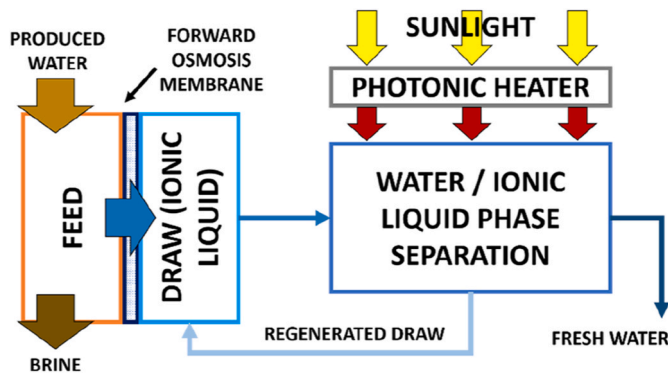


Fig. 1. Setup for water desalination with forward osmosis membrane and photonic heater to regenerate the ionic liquid. Figure inspired from Ref. [5].

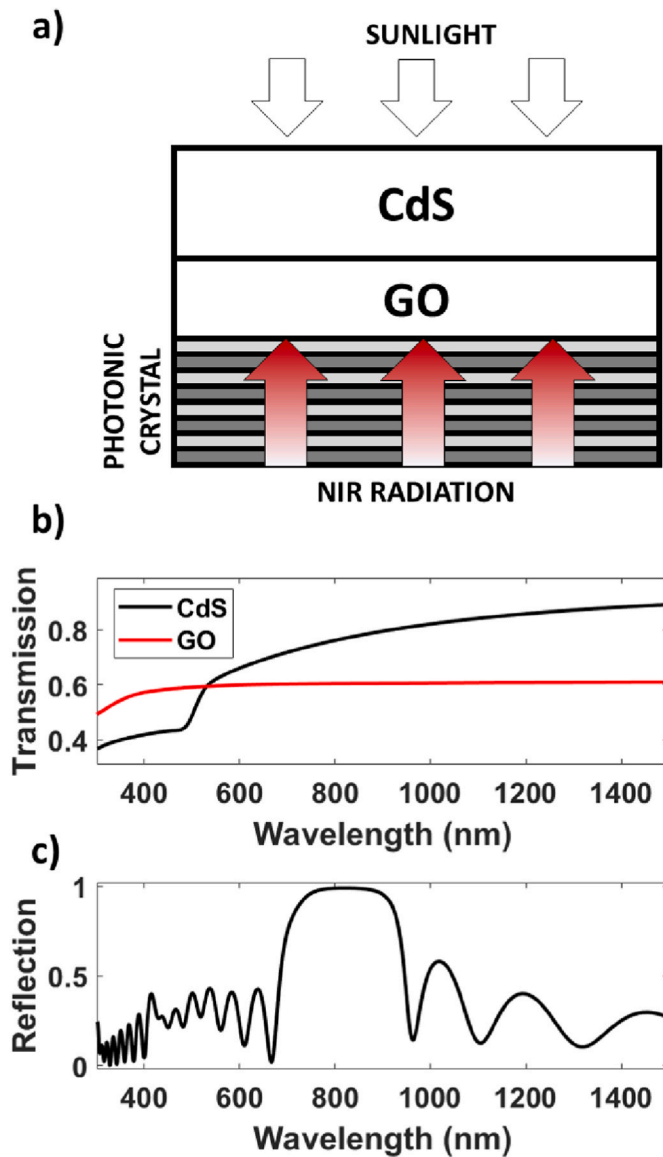


Fig. 2. (b) Transmission spectra of 50 nm thick CdS layer and 12 nm thick graphene oxide layer; (c) reflection of a one-dimensional photonic crystal made of 8 bilayers of 130 nm thick silicon dioxide layers and 97.5 nm thick zirconium dioxide layers. (For interpretation of the references to colour in this figure legend, the reader is referred to the Web version of this article.)

photo-thermal effect occurring in the photonic heater leads to a temperature increase in the module with a subsequent liquid-liquid phase separation. The denser ionic liquid phase settles at the bottom of the module, while the water-rich phase is at the top. The ionic liquid phase is recycled in the forward osmosis module, while the water-rich phase, that contains ionic liquid residuals, undergoes a nanofiltration polishing step at low pressure in order to obtain high quality water [5].

### 1. Photothermal effect (photonic heating) employing photonic crystals

Photo-thermal effect can be achieved also by employing photonic crystals. Thus, properly designed photonic crystals can be used as photonic heaters. Photo-thermal effect with photonic crystals has been exploited for photocatalytic systems. In 2018, Low et al. have reported the fabrication of a titanium dioxide-based photonic crystals for photocatalytic solar fuel production. The photonic band gap of the photonic crystal in the near infrared leads to heat production in the structure with a resulting enhancement of the photocatalytic reaction [17]. Chen et al. report a CdS/graphene oxide (GO) photocatalytic system in which GO absorbs near infrared light, with a subsequent rise of the operating temperature of the system, and a three-dimensional photonic crystal enhances the near infrared absorption of GO [18].

Following the pioneering experiment reported by Chen et al. [18], we propose the substitution of the three-dimensional photonic crystal with a one-dimensional photonic crystal. One-dimensional photonic crystals can be designed with simple theoretical tools and can be fabricated with many experimental techniques, such as sputtering, evaporation, and spin coating [19–21]. In Fig. 2a we sketch the CdS/GO bilayer on top of a one-dimensional multilayer photonic crystal, in which the alternation of layers of two different materials gives rise to the photonic band gap. The light transmission of the films of CdS and GO has been simulated with the transfer matrix method [22–24]. We simulated a system in which light impinges the sample orthogonally with respect to the surface. The studied system is layer above/layer below. For example, in the case of GO, the system is CdS/GO/SiO<sub>2</sub>. The characteristic matrix of the layer can be written as:

$$M = \begin{bmatrix} M_{11} & M_{12} \\ M_{21} & M_{22} \end{bmatrix} = \prod_{k=1}^N \begin{bmatrix} A_k & B_k \\ C_k & D_k \end{bmatrix} \quad (1)$$

With  $A_k = \cos(\frac{2\pi}{\lambda}n_k(\lambda)d_k)$ ;  $B_k = -\frac{i}{n_k(\lambda)}\sin(\frac{2\pi}{\lambda}n_k(\lambda)d_k)$ ;  $C_k = -in_k(\lambda)\sin(\frac{2\pi}{\lambda}n_k(\lambda)d_k)$ ;  $D_k = \cos(\frac{2\pi}{\lambda}n_k(\lambda)d_k)$ .  $n_k(\lambda)$  is the wavelength-dependent refractive index of the  $k$ th layer, while  $d_k$  is the thickness of the  $k$ th layer.  $\lambda$  and  $d_k$  are in nanometers. The light transmission is written as

$$T = \frac{n_A}{n_B} \left| \frac{2n_B}{(M_{11} + M_{12}n_A)n_B + (M_{21} + M_{22}n_A)} \right|^2 \quad (2)$$

And the light reflection is written as

$$R = \left| \frac{(M_{11} + M_{12}n_A)n_B - (M_{21} + M_{22}n_A)}{(M_{11} + M_{12}n_A)n_B + (M_{21} + M_{22}n_A)} \right|^2 \quad (3)$$

In the expressions of transmission and reflection  $n_A$  is the refractive index of the layer above, while  $n_B$  is the refractive index of the layer below.

The thickness of the CdS layer is 50 nm, while the thickness of the GO layer is 12 nm. The real and imaginary parts of the refractive index dispersion of CdS are taken from Refs. [25,26], while the real and imaginary of the (ordinary) refractive index of GO are taken from Ref. [27]. In Fig. 2b we show the simulated transmission curve of a 50 nm thick CdS film (black curve) and the simulated transmission curve of a 12 nm thick GO film (red curve). To the transmission spectrum of GO, an offset of 0.35 of the transmission has been subtracted in order to find a better agreement with the experimental data reported in Ref. [18].

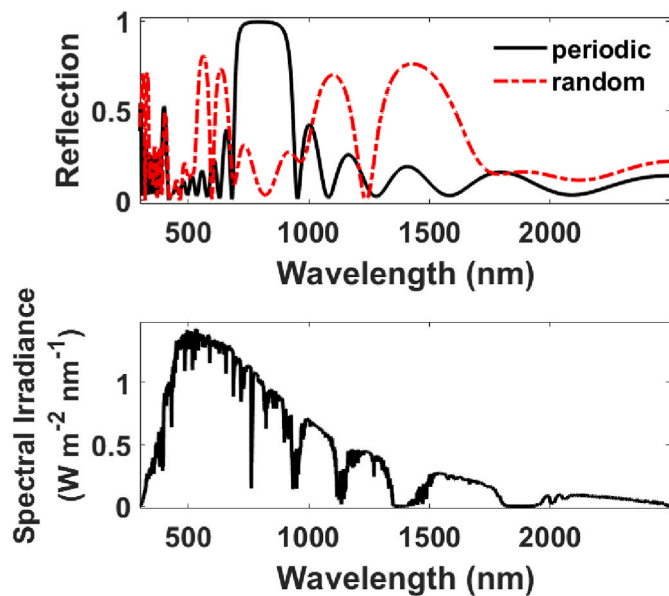


Fig. 3. (above) Reflection of a one-dimensional photonic crystal made of 8 bilayers of silicon dioxide and zirconium dioxide (black solid curve) and of a random photonic structure following the sequence  $ZrO_2/ZrO_2/SiO_2/ZrO_2/ZrO_2/SiO_2/SiO_2/ZrO_2/ZrO_2/ZrO_2/SiO_2/ZrO_2/ZrO_2/SiO_2/ZrO_2/SiO_2$  (red point-dashed curve); (below) Sun spectral irradiance (direct and circumsolar irradiation [30]). (For interpretation of the references to colour in this figure legend, the reader is referred to the Web version of this article.)

Also the light reflection spectrum has been simulated with the transfer matrix method. The photonic crystal is made by 8 bilayers of silicon dioxide and zirconium dioxide. The thickness of the silicon dioxide layers is 130 nm, while the thickness of the zirconium dioxide layers is 97.5 nm. The refractive index dispersion of silicon dioxide is taken from Ref. [28], while the refractive index dispersion is taken from Ref. [29]. In Fig. 2c we show the reflection spectrum of the designed photonic crystal, with a photonic band gap that reflect light in the near infrared region, where the absorption of GO occurs. It is remarkable that with 8 bilayers, which correspond to a total thickness of 1.82  $\mu\text{m}$ , a reflection close to 1 has been achieved.

In Fig. 3 (above) we show the comparison between the light reflection of the periodic  $SiO_2/ZrO_2$  photonic crystal and a random photonic structure that follows the sequence of 16 layers  $ZrO_2/ZrO_2/SiO_2/ZrO_2/ZrO_2/SiO_2/SiO_2/ZrO_2/ZrO_2/ZrO_2/SiO_2/ZrO_2/ZrO_2/SiO_2/ZrO_2/SiO_2$ . As in the periodic photonic crystal, the thickness of the silicon dioxide layers is 130 nm, while the thickness of the zirconium dioxide layers is 97.5 nm. It is remarkable that, with the random sequence, more reflection peaks occur over the range between 300 and 2500 nm. A high reflection of the photonic structure also in the near infrared is important since in this region there is a significant amount of the Sun spectral irradiation (Fig. 3, below) [30].

The reflection of the photonic crystal can be easily tuned via a judicious choice of materials and layer thicknesses. This type of photothermal effect with photonic crystals can be very promising also for water desalination. For the fabrication of real devices, it is certainly necessary to take into account experimental aspects such as the angular dependence of reflection in photonic structures, their roughness, and, finally, their fabrication reproducibility.

## 2. Conclusion

Desalination of water is one of most important contemporary challenges since desalinated water is used for irrigation, industrial processes and in the domestic sector. In this work, we have reported the most significant works on water desalination via membrane distillation

supported by photothermal effects in the water separation processes. We have also envisaged the employment of low-cost and easy-to-design one-dimensional multilayer photonic crystals and random photonic structures as photonic heaters that heat water via a photothermal effect.

## Declaration of competing interest

The authors declare that they have no known competing financial interests or personal relationships that could have appeared to influence the work reported in this paper.

## Data availability

Data will be made available on request.

## Acknowledgement

This project has received funding from the European Research Council (ERC) under the European Union's Horizon 2020 research and innovation programme (grant agreement No. [816313]).

## References

- [1] M.M. Mekonnen, A.Y. Hoekstra, Four billion people facing severe water scarcity, *Sci. Adv.* 2 (2016), e1500323, <https://doi.org/10.1126/sciadv.1500323>.
- [2] A. Alabastri, P.D. Dongare, O. Neumann, J. Metz, I. Adebisi, P. Nordlander, N. J. Halas, Resonant energy transfer enhances solar thermal desalination, *Energy Environ. Sci.* 13 (2020) 968–976, <https://doi.org/10.1039/C9EE03256H>.
- [3] J.J. Urban, Emerging scientific and engineering opportunities within the water-energy nexus, *Joule* 1 (2017) 665–688, <https://doi.org/10.1016/j.joule.2017.10.002>.
- [4] P. Rao, R. Kostecki, L. Dale, A. Gadgil, Technology and engineering of the water-energy nexus, *Annu. Rev. Environ. Resour.* 42 (2017) 407–437, <https://doi.org/10.1146/annurev-environ-102016-060959>.
- [5] A.Z. Haddad, A.K. Menon, H. Kang, J.J. Urban, R.S. Prasher, R. Kostecki, Solar desalination using thermally responsive ionic liquids regenerated with a photonic heater, *Environ. Sci. Technol.* 55 (2021) 3260–3269, <https://doi.org/10.1021/acs.est.0c06232>.
- [6] UN World Water Development Report 2014, UN-water, 2014. <https://www.unwater.org/publications/un-world-water-development-report-2014>. (Accessed 6 September 2022).
- [7] V. Martínez-Alvarez, M.J. González-Ortega, B. Martín-Gorri, M. Soto-García, J. F. Maestre-Valero, 14 - seawater desalination for crop irrigation—current status and perspectives, in: V.G. Gude (Ed.), *Emerging Technologies for Sustainable Desalination Handbook*, Butterworth-Heinemann, 2018, pp. 461–492, <https://doi.org/10.1016/B978-0-12-815818-0.00014-X>.
- [8] /Publications/2012/Mar/Water-Desalination-Using-Renewable-Energy Water desalination using renewable energy, n.d. <https://www.irena.org/publications/2012/Mar/Water-Desalination-Using-Renewable-Energy>. (Accessed 6 September 2022).
- [9] P.D. Dongare, A. Alabastri, S. Pedersen, K.R. Zodrow, N.J. Hogan, O. Neumann, J. Wu, T. Wang, A. Deshmukh, M. Elimelech, Q. Li, P. Nordlander, N.J. Halas, Nanophotonics-enabled solar membrane distillation for off-grid water purification, *Proc. Natl. Acad. Sci. USA* 114 (2017) 6936–6941, <https://doi.org/10.1073/pnas.1701835114>.
- [10] J. Koschikowski, M. Wiegand, M. Rommel, Solar thermal-driven desalination plants based on membrane distillation, *Desalination* 156 (2003) 295–304, [https://doi.org/10.1016/S0011-9164\(03\)00360-6](https://doi.org/10.1016/S0011-9164(03)00360-6).
- [11] L. Zhou, Y. Tan, J. Wang, W. Xu, Y. Yuan, W. Cai, S. Zhu, J. Zhu, 3D self-assembly of aluminium nanoparticles for plasmon-enhanced solar desalination, *Nat. Photonics* 10 (2016) 393–398, <https://doi.org/10.1038/nphoton.2016.75>.
- [12] P.D. Dongare, A. Alabastri, O. Neumann, P. Nordlander, N.J. Halas, Solar thermal desalination as a nonlinear optical process, *Proc. Natl. Acad. Sci. USA* 116 (2019) 13182–13187, <https://doi.org/10.1073/pnas.1905311116>.
- [13] S. John, Strong localization of photons in certain disordered dielectric superlattices, *Phys. Rev. Lett.* 58 (1987) 2486–2489, <https://doi.org/10.1103/PhysRevLett.58.2486>.
- [14] E. Yablonovitch, Inhibited spontaneous emission in solid-state physics and electronics, *Phys. Rev. Lett.* 58 (1987) 2059–2062, <https://doi.org/10.1103/PhysRevLett.58.2059>.
- [15] J.D. Joannopoulos (Ed.), *Photonic Crystals: Molding the Flow of Light*, second ed., Princeton University Press, Princeton, 2008.
- [16] H. Sayed, T.F. Krauss, A.H. Aly, Versatile photonic band gap materials for water desalination, *Optik* 219 (2020), 165160, <https://doi.org/10.1016/j.ijleo.2020.165160>.
- [17] J. Low, L. Zhang, B. Zhu, Z. Liu, J. Yu, TiO<sub>2</sub> photonic crystals with localized surface photothermal effect and enhanced photocatalytic CO<sub>2</sub> reduction activity, *ACS Sustainable Chem. Eng.* 6 (2018) 15653–15661, <https://doi.org/10.1021/acssuschemeng.8b04150>.

- [18] Y. Chen, J. Fang, B. Dai, J. Kou, C. Lu, Z. Xu, Photothermal effect enhanced photocatalysis realized by photonic crystal and microreactor, *Appl. Surf. Sci.* 534 (2020), 147640, <https://doi.org/10.1016/j.apsusc.2020.147640>.
- [19] S. Colodrero, M. Ocaña, H. Míguez, Nanoparticle-based one-dimensional photonic crystals, *Langmuir* 24 (2008) 4430–4434, <https://doi.org/10.1021/la703987r>.
- [20] D.P. Puzzo, L.D. Bonifacio, J. Oreopoulos, C.M. Yip, I. Manners, G.A. Ozin, Color from colorless nanomaterials: bragg reflectors made of nanoparticles, *J. Mater. Chem.* 19 (2009) 3500–3506, <https://doi.org/10.1039/B903229K>.
- [21] P. Lova, G. Manfredi, D. Comoretto, Advances in functional solution processed planar 1D photonic crystals, *Adv. Opt. Mater.* 6 (2018), 1800730, <https://doi.org/10.1002/adom.201800730>.
- [22] M. Born, E. Wolf, A.B. Bhatia, P.C. Clemmow, D. Gabor, A.R. Stokes, A.M. Taylor, P.A. Wayman, W.L. Wilcock, *Principles of Optics: Electromagnetic Theory of Propagation, Interference and Diffraction of Light*, seventh ed., Cambridge University Press, 1999 <https://doi.org/10.1017/CBO9781139644181>.
- [23] A. Chiasera, F. Scotognella, L. Criante, S. Varas, G.D. Valle, R. Ramponi, M. Ferrari, Disorder in photonic structures induced by random layer thickness, *Sci. Adv. Mater.* 7 (2015) 1207–1212, <https://doi.org/10.1166/sam.2015.2249>.
- [24] G.M. Paternò, L. Moscardi, S. Donini, D. Ariodanti, I. Kriegel, M. Zani, E. Parisini, F. Scotognella, G. Lanzani, Hybrid one-dimensional plasmonic–photonic crystals for optical detection of bacterial contaminants, *J. Phys. Chem. Lett.* 10 (2019) 4980–4986, <https://doi.org/10.1021/acs.jpclett.9b01612>.
- [25] R.E. Treharne, A. Seymour-Pierce, K. Durose, K. Hutchings, S. Roncallo, D. Lane, Optical design and fabrication of fully sputtered CdTe/CdS solar cells, *J. Phys.: Conf. Ser.* 286 (2011), 012038, <https://doi.org/10.1088/1742-6596/286/1/012038>.
- [26] RefractiveIndex.INFO - refractive index database, n.d. <https://refractiveindex.info/>. (Accessed 15 November 2019).
- [27] S. Schöche, N. Hong, M. Khorasaninejad, A. Ambrosio, E. Orabona, P. Maddalena, F. Capasso, Optical properties of graphene oxide and reduced graphene oxide determined by spectroscopic ellipsometry, *Appl. Surf. Sci.* 421 (2017) 778–782, <https://doi.org/10.1016/j.apsusc.2017.01.035>.
- [28] I.H. Malitson, Interspecimen comparison of the refractive index of fused silica, *J. Opt. Soc. Am.*, JOSA. 55 (1965) 1205–1209, <https://doi.org/10.1364/JOSA.55.001205>.
- [29] D.L. Wood, K. Nassau, Refractive index of cubic zirconia stabilized with yttria, *Appl. Opt.*, AO. 21 (1982) 2978–2981, <https://doi.org/10.1364/AO.21.002978>.
- [30] Reference air mass 1.5 spectra, n.d. <https://www.nrel.gov/grid/solar-resource/spectra-am1.5.html>. (Accessed 18 September 2022).